

PLASMA DYNAMICS



## VIII. PLASMA PHYSICS\*

### Academic and Research Staff

Prof. S. C. Brown  
Prof. W. P. Allis

Prof. G. Bekefi  
Prof. J. C. Ingraham  
Dr. G. Lampis

J. J. McCarthy  
W. J. Mulligan

### Graduate Students

M. L. Andrews  
D. L. Flannery  
E. V. George

W. H. Glenn, Jr.  
P. W. Jameson  
R. L. Kronquist  
D. T. Llewellyn-Jones

G. L. Rogoff  
D. W. Swain  
F. Y-F. Tse

### A. APPROXIMATE SOLUTION OF THE COLLISIONLESS PLASMA-SHEATH EQUATION FOR BEAM-GENERATED PLASMA IN A PLANE GEOMETRY

The collisionless plasma-sheath equation for beam-generated plasma in a plane geometry has the form<sup>1</sup>

$$\frac{a^2}{2} [S''(x)]^{-1} + \beta + e^{-x} = \int_0^x [x-\xi]^{-1/2} S'(\xi) d\xi, \quad (1)$$

where

$$a \equiv \frac{(M/m)^{1/2} v}{\omega_p} \quad (2)$$

is a small parameter with typical values between  $10^{-3}$  and  $10^{-1}$ , and  $\beta \equiv n_b/n_{e0}$  is the ratio of the beam electron density to the plasma electron at the center. With the boundary condition  $\left[\frac{dS}{dx}\right]_{x=0}^{-1} = 0$ , Eq. 1 can be integrated analytically with respect to  $x$  to give

$$\frac{a^2}{4} [S'(x)]^{-2} + H_0(x) = 2 \int_0^x [x-\xi]^{1/2} S'(\xi) d\xi, \quad (3)$$

where  $H_0(x) = \beta x + 1 - e^{-x}$ .

Integrating the right-hand side of Eq. 3 by parts and denoting  $S$  by  $S_a$  for  $a \neq 0$  yields the plasma-sheath equation in the form

$$\frac{a^2}{4} [S'_a(x)]^{-2} + H_0(x) = \int_0^x [x-\xi]^{-1/2} S_a(\xi) d\xi. \quad (4)$$

For  $a = 0$ , and since  $H(0) = 0$ , Eq. 4 is an Abel's integral equation with the solution

---

\*This work is supported by the United States Atomic Energy Commission (Contract AT (30-1)-1842).

(VIII. PLASMA PHYSICS)

$$S_0(x) = \frac{1}{\pi} \frac{d}{dx} \int_0^x (x-\xi)^{-1/2} H_0(\xi) d\xi. \quad (5)$$

By changing  $\xi \rightarrow \xi - x$ , Eq. 5 gives

$$S_0(x) = \frac{1}{\pi} \int_0^x (x-\xi)^{-1/2} H_0'(\xi) d\xi. \quad (6)$$

For  $H_0(x) = \beta x + (1-e^{-x})$ , Eq. 6 reduces to the solution derived previously by Harrison and Thompson<sup>2</sup> ( $\beta=0$ ):

$$S_0(x) = \frac{2}{\pi} x^{1/2} [\beta + B(x)], \quad (7)$$

where

$$B(x) \equiv \int_0^1 \exp[x^2(\xi^2-1)] d\xi$$

$$\longrightarrow \begin{cases} 0 & \text{as } x \rightarrow 0 \\ \frac{1}{2x} & \text{as } x \rightarrow \infty \end{cases} \quad (8)$$

We found it convenient to use the function  $B(x)$  rather than the Dawson function that Harrison and Thompson used. The function  $B(x)$  is related to Dawson function by the relation

$$x^{1/2} B(x) \equiv e^{-x} D(x^{1/2}). \quad (9)$$

For  $a \neq 0$  we shall separate solution into two regions. For the inner solution we define

$$R_a(x) \equiv S_a(x) - S_0(x) \quad \text{for } 0 \leq x \leq x_c - \delta,$$

where  $x_c = 0.3444$  with  $S_0'(x_c) = 0$ , and  $\delta$  is a positive number such that  $R_a(x) \ll S_0(x)$  in this region.

Then the integro-differential equation satisfied by  $R_a(x)$  has the form

$$\frac{a^2}{4} [S_0'(x) + R_a'(x)]^{-2} = \int_0^x (x-\xi)^{-1/2} R_a(\xi) d\xi. \quad (10)$$

Equation 10 also has the form of the Abel's equation with the solution

$$R_a(x) = \frac{a^2}{4\pi} \int_0^x (x-\xi)^{-1/2} \frac{d}{d\xi} \left\{ [S_0'(\xi) + R_a'(\xi)]^{-2} \right\}. \quad (11)$$

Since  $R_a'(\xi) \ll S_0'(\xi)$  in this region, Eq. 11 can be written

$$R_a(x) \approx \frac{a^2}{2\pi} \int_0^x \frac{(x-\xi)^{-1/2} |S_0''(\xi)|}{[S_0'(\xi)]^3} d\xi. \quad (12)$$

Equation 12 thus gives  $R_a(x)$  in terms of known functions. Note that Eq. 12 is good only for  $x \leq x_c - \delta$  because at  $x = x_c$   $S'_0$  is zero. For the outer solution we define

$$S_a(x) \equiv S_a(x_c - \delta) + af_a(x) \quad \text{for } x > x_c - \delta, \quad (13)$$

where  $S_a(x_c - \delta)$  is given by the inner solution. With  $H_0(x) = \int_0^x (x-\xi)^{-1/2} S_0(\xi) d\xi$  as required by Eq. 4, and if we neglect  $R_a(x)$  for the inner region  $0 \leq x \leq x_c - \delta$ , Eq. 4 becomes

$$\begin{aligned} \frac{1}{4} [f'_a(x)]^{-2} &\approx \int_0^{x_c - \delta} (x-\xi)^{-1/2} S_0(\xi) d\xi \\ &+ \int_{x_c - \delta}^x (x-\xi)^{-1/2} [S_a(x_c - \delta) + af_a(\xi)] d\xi \\ &- \int_0^x (x-\xi)^{-1/2} S_0(\xi) d\xi \\ &= \int_{x_c - \delta}^x (x-\xi)^{-1/2} [S_a(x_c - \delta) + af_a(\xi) - S_0(\xi)] d\xi. \end{aligned} \quad (14)$$

Assume that  $af_a(\xi) \ll S_a(x_c - \delta) - S_0(\xi)$  for small  $a$ . Then Eq. 14 gives

$$f_a(x) = \frac{1}{2} \int_{x_c - \delta}^x \frac{d\xi}{\sqrt{\int_{x_c - \delta}^{\xi} (\xi-\eta)^{-1/2} [S_a(x_c - \delta) - S_0(\eta)] d\eta}}. \quad (15)$$

Equation 15 gives  $f_a(x)$  in terms of known functions. In this particular form, however, it is not very useful for computational purpose and more work is being done along this line.

It should be stated that the assumption  $af_a(\xi) \ll S_a(x_c - \delta) - S_0(\xi)$  is rigorously justifiable but is omitted here for the sake of brevity.

F. Y-F. Tse

#### References

1. D. A. Dunn and S. A. Self, J. Appl Phys. 35, 113 (1964).
2. E. R. Harrison and W. B. Thompson, Proc. Phys. Soc. (London) 72, 2145 (1959).

(VIII. PLASMA PHYSICS)

B. LASER BREAKDOWN

A laser breakdown experiment in gas is being performed. The plasma is produced by focussing in Helium with a 68-mm focal length lens, a laser beam of 40-MW average power, and 50-nsec width, produced by a switched ruby laser (see Fig. VIII-1). The

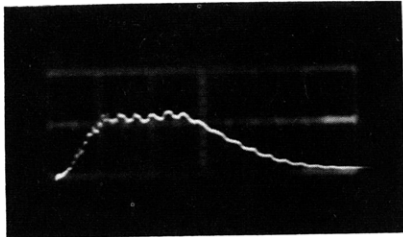


Fig. VIII-1. Typical pulse from the ruby laser. Total energy: 2.1 joules.

VERTICAL : gv/div  
HORIZONTAL : 20 nsec/div

Helium can be pressured up to 10 atm in a stainless-steel box with quartz windows to which a light dump has been connected for quenching the part of the ruby beam not absorbed by the plasma.<sup>1-7</sup>

The plasma spark produced in the focus of the lens is cylindrically shaped with the axis in the direction of the ruby beam. The plasma is being studied by crossing it with

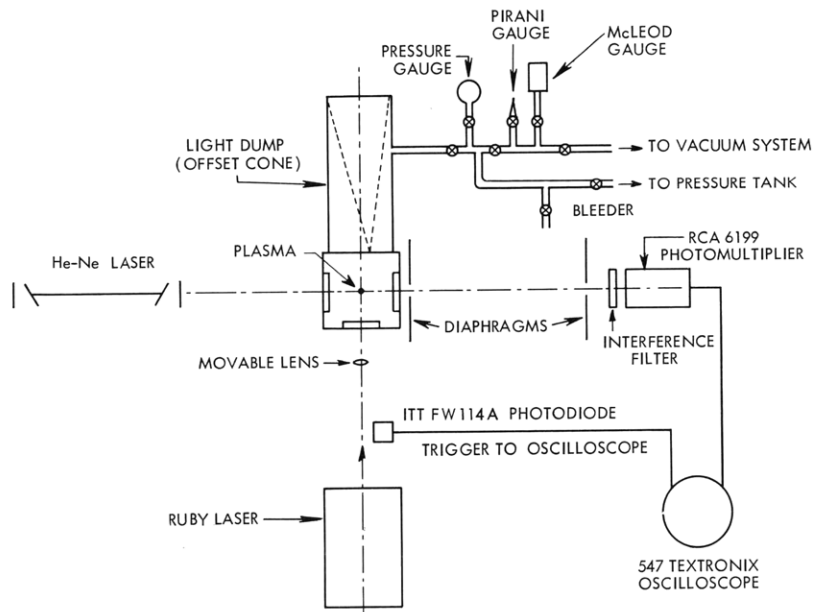


Fig. VIII-2. Experimental arrangement.

the light of a Helium-Neon laser, whose beam is at an angle of  $90^\circ$  with the ruby beam. See Fig. VIII-2.

The gas laser light emerging from the spark is detected together with the emission from the plasma by a photomultiplier tube (RCA 6199) in front of which a diaphragm system and a sharp interferential filter ( $7 \text{ \AA}$  half-width centered at  $6328 \text{ \AA}$ ) have been introduced. The 547 Textronix oscilloscope is triggered by an ITT FW114A photodiode looking at the side of the ruby beam and collecting the Rayleigh scattered signal. Figure VIII-3 shows the combination of the signals caused by the emission from the plasma and the light from the gas laser, which has crossed the spark. On the left is shown the level of the steady-state value of the power  $P_\ell$  from the gas laser. When the breakdown happens, the pulse presents a fast rise time  $\approx 30 \text{ nsec}$  resulting from the strong emission from the plasma. The emission then decays (see Fig. VIII-4) and meanwhile the He-Ne laser light is being absorbed. This causes the pulse amplitude to decrease back to the initial value  $P_\ell$  and beyond. When the signal equals the initial steady-state value of the He-Ne laser (before the breakdown) the following equality is verified:

$$P_\ell \cdot e^{-2aR} + P_{\text{plasma}}(R, T) = P_\ell, \quad (1)$$

where  $P_\ell$  is the power of the He-Ne laser which reaches the photomultiplier tube when there is no plasma in the geometry of the experiment;  $a$  is the absorption coefficient of the plasma for the laser frequency;  $R$  is the radius of the cylindrically shaped bubble of plasma;  $P_\ell e^{-aL}$  is then the power from the gas laser attenuated by the plasma;  $P(R, T)$  is the power emitted by the plasma, reaching the photomultiplier tube in the band of the filter and in the geometry of the experiment; and  $T$  is the temperature of the plasma, which is supposed to be homogeneous.

Figure VIII-4 shows the shape of the emission from the plasma in the band of the interferential filter. This picture was obtained by blinding the gas laser beam while the breakdown was being produced. By subtracting from the combination of the emission and absorption signals (Fig. VIII-3) the signal of the emission alone (Fig. VIII-4), both being detected in the same geometry, the optical thickness,  $aL$ , of the plasma is thus determined at every time of the plasma's life.

This subtraction of data taken during different sparks, is allowed by the fairly good reproducibility of the emission and absorption. By calculating theoretically, as a function of the radius and of the temperature of the plasma, the value  $P_{\text{plasma}}(T, R)$  of the emitted power impinging on the photomultiplier tube, and knowing  $R$  through measurements of the velocity of the radial expulsion of the bubble, the temperature  $T$  can be calculated at the instant  $t^*$  in which relation (1) is true, as a function of  $P_\ell$ .  $P_\ell$  is measured by substituting for the photomultiplier a colorimetric cell (401 spectra physics power meter), which calibrates the whole geometry. By using different values of the

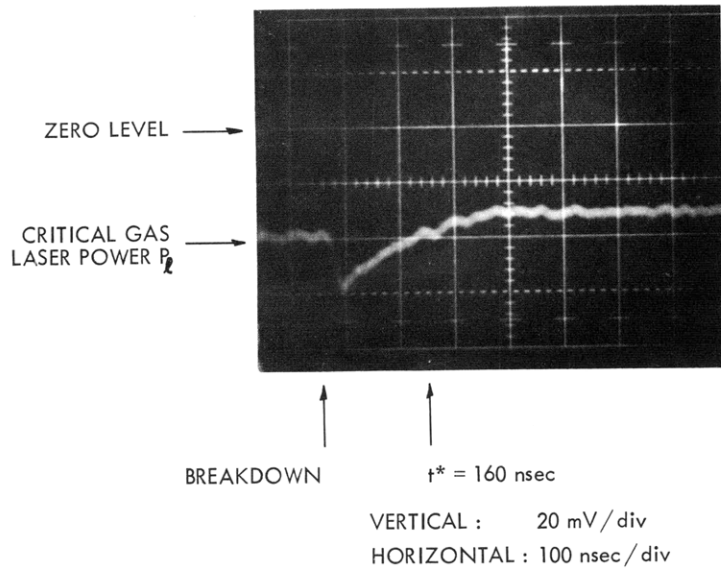


Fig. VIII-3.  
Typical emission curve from the plasma.

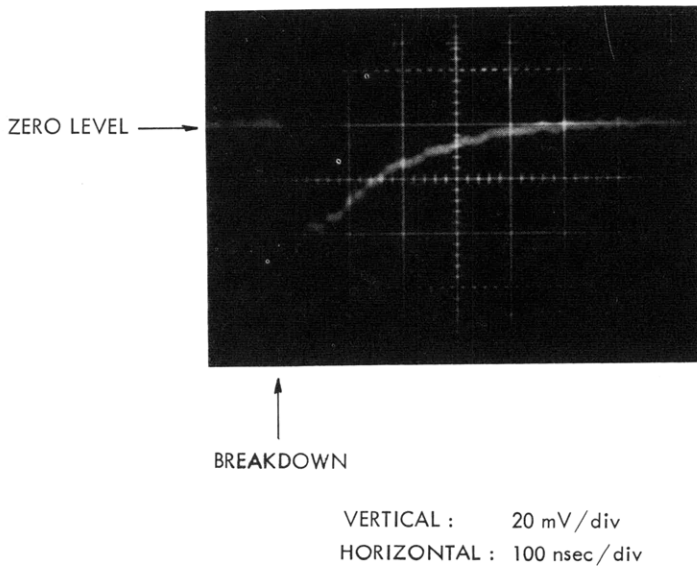


Fig. VIII-4. Typical absorption curve.

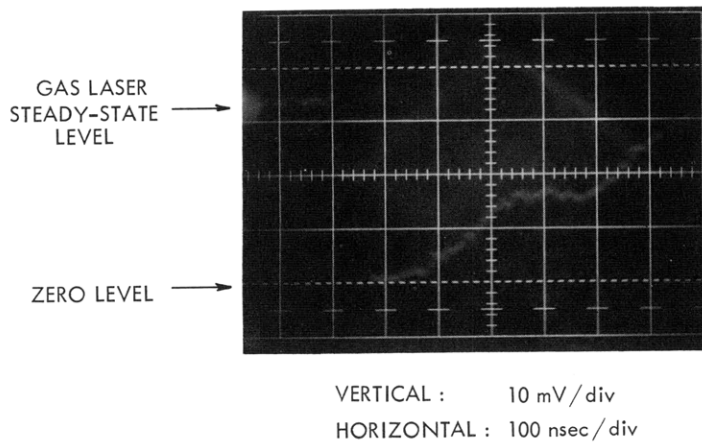


Fig. VIII-5.  
Signal combination of the power signals from the plasma and from the gas laser.

power of the gas laser, the instant  $t^*$  can be shifted and a sampling of the temperature of the plasma can be made. Thus far, samplings between 100 nsec and 1.2  $\mu$ sec have been obtained. By using very small-diameter diaphragms for limiting the light reaching the photomultiplier tube, it is possible to eliminate completely the contribution from the plasma emission and allow only the detection of the gas laser beam. In this situation, clear pictures of the absorption of the He-Ne laser have been obtained (Fig. VIII-5), which show that the total absorption takes place in the early stages of the life of the plasma.

Measurements of the radial expansion velocity are being made by offsetting by a known distance the helium-neon beam in a plane normal to the ruby beam and measuring the delay in the absorption effect.

By moving in known amounts the position of the lens, focussing the ruby laser, and measuring the delay in the absorption on the helium beam, measurements of the expansion velocity along the cylindrical axis of the plasma are being made; previous measurements give values of  $2.5 \times 10^5$  cm/sec at 11.5 atm pressure. Theoretical work is under way on the calculation of  $P_{\text{plasma}}(R, T)$ .

Further experimental work will be related to the study of the dependence of  $T$  on the pressure of the gas and on improving the geometry of the detection.

When the diameter of the plasma is large with respect to the acceptance of the diaphragms, a simplification made by averaging on the solid angle through which the beams from the plasma spark are received by the photomultiplier gives

$$P_{\ell} e^{-aL} + \xi B(T) (1 - e^{-aL}) = P_{\ell}, \quad (2)$$

where  $\xi$  is a constant depending on the geometry and on the interference filter characteristics, and  $B(T)$  is the Planck function.

The factor  $(1 - e^{-aL})$  drops out and the quantity  $B(T)$  is proportional to the measured  $P_{\ell}$ .

$$B(T) = \frac{P_{\ell}}{\xi}.$$

At 110 nsec after breakdown, a temperature of 4 ev has been calculated in this way.

G. Lampis

#### References

1. S. L. Mandel'shtam et al., Soviet Phys. - JETP 22, No. 1 (January 1966).
2. Ya. Zel'dovich and Yu. Raizer, Soviet Phys. - JETP 20, No. 3 (March 1965).
3. Yu. Raizer, Soviet Phys. - JETP 21, No. 5 (November 1965).
4. G. Akor'yan and M. S. Rabinovich, Soviet Phys. - JETP 21, No. 1 (July 1965).
5. D. Ryutov, Soviet Phys. - JETP 20, No. 6 (July 1965).
6. R. G. Meyerand, Jr. and A. F. Haught, Phys. Rev. Letters 1, 9 (November 1, 1963).
7. R. G. Meyerand, Jr. and A. F. Haught, Phys. Rev. Letters 13, 1 (July 6, 1964).

